# Preparation of Monodispersed and Lipophilic Attapulgite and Polystyrene Nanorods via Surface-Initiated Atom Transfer Radical Polymerization

**Hong Zhang,[1,2] Weichun Ye,[1] Feng Zhou[1,2]**

[1]*College of Chemical Engineering, Northwest University for Nationalities, Lanzhou 730030, China*
[2]*State Key Laboratory of Solid Lubrication, Lanzhou Institute of Chemical Physics, Chinese Academy of Sciences, Lanzhou 730000, China*

Received 9 October 2009; accepted 16 January 2010
DOI 10.1002/app.34337
Published online 6 July 2011 in Wiley Online Library (wileyonlinelibrary.com).

**ABSTRACT:** A new kind of initiator, 3-(2-bromo-2-methylacryloxy)propyltriethysiliane (MPTS-Br), was prepared with a simply hydrobrominated commercial silane coupling agent (3-methacryloxy-proplytriethysilane, MPTS). It has been one-step self-assemble onto the surface of attapulgite (ATP) nanorods in the dispersion system, and by using this initiator-modified nanorod (MPTS-Br-modified ATP nanoparticles, ATP-MPTS-Br) as macroinitiator for atom transfer radical polymerization (ATRP). Structurally well-defined homopolymer polystyrene (PS) and block polymer poly(styrene-*b*-methyl methacrylate) (PS-*b*-PMMA) chains were then grown from the needle-shaped nanorods surface to yield monodispersed nanorods composed of ATP core and thick-coated polymer shell (ATP and PS). The graft polymerization parameters exhibited the characteristics of a controlled/"living" polymerization. The PS-grafted ATP nanorods could be dispersed well in organic solvent with nanoscale. © 2011 Wiley Periodicals, Inc. J Appl Polym Sci 122: 2876–2883, 2011

**Key words:** attapulgite; surface-initiated; atom transfer radical polymerization; core-shell nanorods

## INTRODUCTION

The surface functionalizations of nanomaterials by grafting of polymer are expected to play important roles in the designing of novel organic/inorganic nanocomposite materials. The grafting of polymer onto inorganic particles, such as silica, clay, carbon black, and ferrite, is an effective means to improve surface properties, because the surface-grafted polymer chain can interfere with the aggregation of these particles and increase their surface affinity for organic solvents and polymer matrixes.[1–4] However, conventional surface-initiated free radical polymerization, especially when confined to a thin layer, leads to a wide molecular weight distribution of the grafted polymer, largely due to termination reaction.[5] Moreover, this approach is not suitable for preparing block copolymer. So, there has been increasing research activity concerning the use of "living" polymerization, such as cationic,[6,7] anionic,[8,9] ring-opening,[10] nitroxide-mediated,[11,12] reversible addition fragmentation chain transfer,[13] and atom transfer radical polymerization (ATRP),[14–19] to grow polymer from the nanoparticle surface. Of these methods, surface-initiated atom transfer radical polymerization (SI-ATRP) is preferred, because it does not require stringent conditions and is tolerant of functional groups and impurities that are detrimental to other "living" polymerization.[20] ATRP is a robust and versatile technique to accurately control the chain length and polydispersity index (PDI = $M_w/M_n$) of the polymer and can be used to synthesize well-defined copolymer. There are a number of reports in the literatures of studying the mechanism, monomer, initiator, ligand and metal catalyzer, and some comprehensive reviews in this field have been published as well.[21–24]

Attapulgite (ATP) is a hydrated magnesium aluminum silicate, which is a type of natural fibrillar clay mineral of densely packed fibrous clusters in appearance with the diameter of a single rod less than 100 nm and the length of a rod from several hundreds of nanometers to several micrometers. Different from the spherical or layered silicates nanoparticles reported, the needle-shaped particle has the enormous aspect ratio; a strong van der Waals attraction force appeared among ATPs, resulting in

*Correspondence to:* F. Zhou (zhouf@lzb.ac.cn).
Contract grant sponsor: Chinese Academy of Sciences (Hundred Talents Program).
Contract grant sponsor: NSFC; contract grant numbers: 50721062 and 50835009.
Contract grant sponsor: Northwest University for Nationalities (Innovation Research Fund for Young Scholars); contract grant number: XBMU-2008-BD-87.

the formation of large compact bundles crystals so that it is difficult to be dispersed well in organic solvent with nanoscale or single rod. Nevertheless, the high aspect ratio of the ATP fibers with good mechanical strength and thermal stability make it very useful in reinforcement of polymeric materials as reinforcing fillers.[25–32] In the preparation of polymer/ATP nanocomposite, the most important step is the activation of the ATP fibers, which enables active organic groups or polymer (to react or graft) onto the surface of the fibers.[31] After surface activation, the organic groups or the long polymer chains could be efficient in preventing ATPs from flocculating in polymer matrix, improving its dispersibility in polymer matrix.

In this work, a novel simple method was developed for immobilizes the α-bromoester initiator on needle-shaped ATP nanoparticles. The commercial silane coupling agent, 3-methacryloxyproply-triethysilane (MPTS), has been simply modified by hydrobromination to form 3-(2-bromo-2-methylacryloxy)-propyltriethy-siliane (MPTS-Br), followed by one-step self-assemble initiator onto the surface of ATP nanoparticles according to conventional classic method, using reactive-OH groups on ATP surface, and to form the MPTS-Br-modified ATP nanoparticles (ATP-MPTS-Br). The tertiary α-bromoester on the surface of the nanoparticles could serve as ATRP initiator. Compared with surface initiator was immobilized onto nanoparticles usually in a multistep heterogeneous process mentioned above,[14–24,33,34] which technique often leads to low-grafting density and low-film thickness, because the multistep heterogeneous process give rise to the low density of the initiator on the nanoparticles. Surface-tethered α-bromoester initiator with our method only underwent one-step heterogeneous process, the initiator density on the ATP nanoparticles was high. Therefore, structurally well-defined, densely grafted, and thick-coated polymer layer by SI-ATRP could be obtained. The morphology and the dispersibility in organic solvent of the polymer-graft ATP particles and some properties of polymer brushes were discussed.

## EXPERIMENTAL

### Materials and methods

Styrene (St) and methyl methacrylate (MMA) were purchased from Lanzhou Chemical Corporation (Lanzhou, China) and purified by treating with 5 wt % aqueous NaOH to remove the inhibitor and then washed with distilled water until pH = 7, which was dried over by anhydrous calcium chloride for 24 h and then stored at low temperature before use. ATP nanofibrillar clay with the average diameter of 325 meshes was provided by Gansu ATP (Gansu, China). It was dried in a vacuum at 110°C for 48 h before use. MPTS (Gaizhou Chemical Industrial, Liaoning, China) and 2,2′-bipyridine (bipy) (Tianjin Chemical, Tianjin, China) were used as received. Cu(I)Br (Tianjin Chemical, Tianjin, China) was purified by stirring in acetic acid, filtered, washed with ethanol, and dried in turn. Hydroquinone (Beijing Chemical Factory, Beijing, China), hydrogen fluoride (HF), ethanol, toluene, tetrahydrofuran (THF), dichloromethane, and all other reagents used were analytical grade.

### Preparation of the macroinitiator and graft polymerization

#### Preparation and immobilization of initiator

The macroinitiator, ATP-MPTS-Br, was prepared as the following procedure: 30 mL (0.11 μmol) of MPTS was dissolved in 150 mL of anhydrous dichloromethane and placed in a 500-mL three-necked flask with a magnetic stirrer. Hydroquinone (0.3 g) was added as an inhibitor and a little *p*-methylbenzene sulfonic acid was added as the catalyst. Dry HBr gas was introduced into the mixture in an ice water bath. The mixture was stirred at 0°C for 2 h before the flow was stopped, then the HBr-saturated mixture was sealed and stirred overnight. The MPTS-Br dissolved in dichloromethane was obtained. Then, 2-g ATP nanofibrillar was charged, and the mixture was dispersed with ultrasonic vibration for 30 min, and then stirred at room temperature for 12 h. After the self-assembly procedure, the mixture was centrifuged, and the precipitate was washed with dichloromethane and ethanol thoroughly. The resulting precipitation ATP nanofibrillar modified by MPTS-Br, ATP-MPTS-Br, were immediately used for surface polymerization after being dried in vacuum at the room temperature.

#### Synthesis of polymer brushes

A typical polymerization process St from the surface of the ATP macroinitiator was described as follows: 0.8-g ATP-MPTS-Br nanoparticles and 80-mL toluene were charged into a 150-mL dry flask equipped with a reflux condenser and a magnetic stirrer. The flask was ultrasonicated for 30 min, 0.187 g (1.2 mmol) bipy, and 0.063 g (0.44 mmol) Cu(I)Br were added to this flask after that. It was subsequently evacuated and flushed with nitrogen three times and then degassed monomer, St, 6 mL (5.5 g) was injected. The mixture was stirred rapidly under nitrogen and placed in oil bath at 110°C. Parts of the mixture were taken out after a certain polymerization time. The products were separated by centrifugation and washed thoroughly with toluene, ethanol, and water in turn, which removed unreacted St, ungrafted

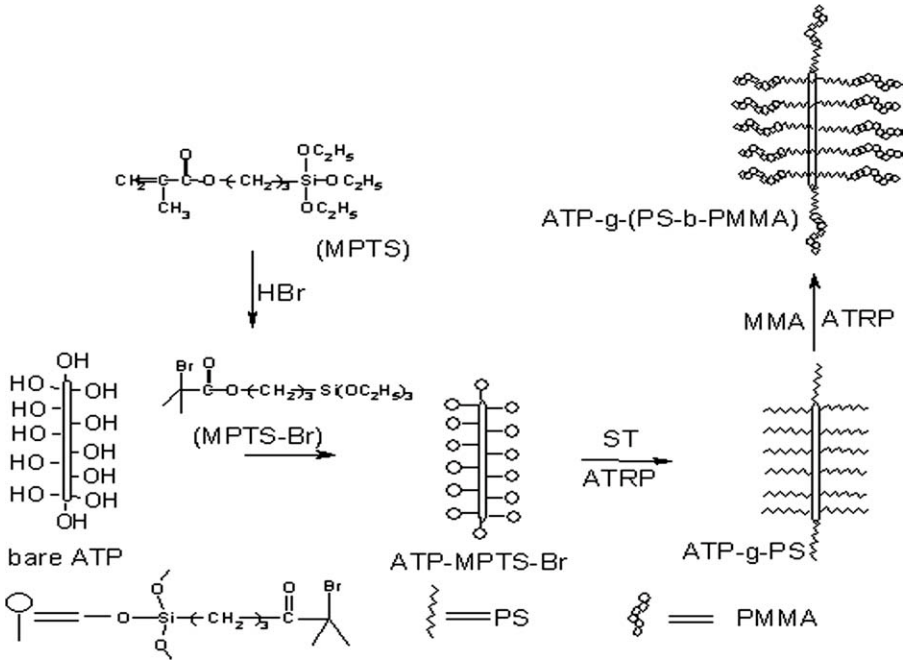


**Scheme 1** The self-assembly of the macroinitiator and synthetic rout to the ATP-*g*-PS and ATP-*g*-(PS-*b*-PMMA).

polystyrene (PS), and virtually all the remaining Cu-salts. The final products, ATP-*g*-PS, was dried in vacuum at room temperature.

Hybrid nanocomposite, ATP-*g*-(PS-*b*-PMMA), possessing PS-*b*-PMMA block copolymer was prepared using the similar general procedure as described above, except with ATP-*g*-PS hybride nanorods as macroinitiator to SI-ATRP of MMA.

### Cleavage of the graft polymer from the ATP nanoparticles

PS chains grown from the ATP nanorods were cleaved as describe in the reference procedure:[35] 0.4 g of sample was vigorously stirred in a poly(ethylene) flask containing 14-mL toluene, 10-mL 20 wt % aqueous HF solution, along with Aliquat 336 as a phase transfer catalyst. After 2 h, the aqueous layer was removed, and 10-mL 20 wt % HF containing Aliquat 336 was added and stirred for another 2 h. This procedure was repeated until no impurities could be detected by gel permeation chromatography (GPC) measurement. The PS contained in organic layer was recovered by precipitation into methanol and vacuum filtration through fine-grained glass frit, yielding white powder.

### Characterization

Elemental analysis (EA) of C, N, and H was performed on Elementar Vario EL instrument. Fourier transform infrared spectra (FTIR) were performed using a Bio-RA FTS-165 spectrometer. X-ray photoelectron spectroscopy (XPS) measurements were carried out with a PHI-5702 multifunctional spectrometer. The morphologies of the polymer graft nanorods were observed with a HITACHI H-600 transmission electro microscopy (TEM), which was used operating at 100 kV. The samples dispersions were diluted and ultrasonized and then dried onto carbon-coated copper grids to examine. The glass transition temperature ($T_g$) were obtained by the differential scanning calorimetry (DSC) analysis with a Perkin-Elmer Saphire, between 30 and 190°C at a heating rate of 10°C $min^{-1}$. A nitrogen purge was applied. Molecular weight and molecular weight distribution were measured by GPC on a Waters GPCV2000 system using THF as eluent.

## RESULTS AND DISCUSSION

### Preparation and immobilization of initiator

Scheme 1 illustrated the self-assembly procedures of the macroinitiator, ATP-MPTS-Br, and the ATRP "grafting from" approach used to synthesize the tethered polymer brushes. First, a monolayer of ATRP initiator was deposited on the ATP nanorods surface by cohydrolyzing the triethyoxysilane of MPTS-Br with the surface reactive-OH groups on the ATP nanorods. Unreacted initiator was washed from the particles by repeat suspension, centrifugation, and decanting of the supernatant. The FTIR spectra (Fig. 1) of the immobilized initiator (ATP-MPTS-Br) showed a C—H stretching vibration at 2950 $cm^{-1}$, which was not present in spectrum of unmodified ATP nanorods. Comparing with the

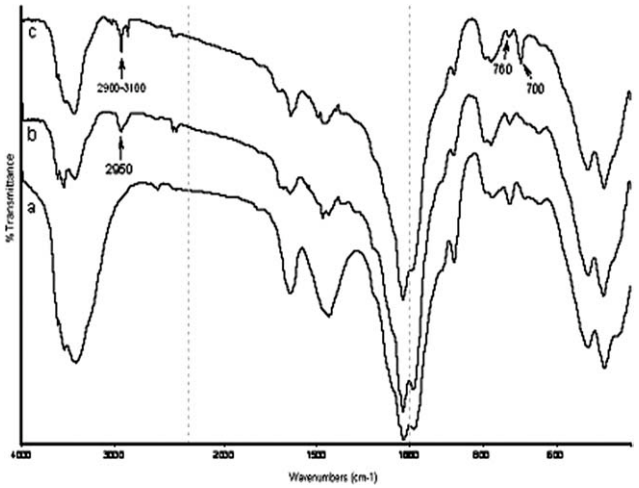


**Figure 1** FTIR spectra of (a) bare ATP, (b) ATP-MPTS-Br, and (c) ATP-*g*-PS.

naked ATP, the peak shape of ATP-MPTS-Br around 1600–1750 $cm^{-1}$ area attributed to C=O stretching vibration were also changed. The XPS was also used to confirm the formation of the initiator monolayer. Figure 2(a) showed the survey scan spectrum of the modified ATP nanoparticles. The successful immobilization of bromoester initiators on the surface was verified by the appearance of the peak of Br3d (71 ev). Beside the peak of Br3d was observed around 71 ev [Fig. 2(a,b)], Figure 2(c) showed the peak of Si2p of ATP-MPTS-Br could be curve fitted with two peak components having binding energy at 103.3 and 101.6 ev, attributable to the Si—O and Si—C species, respectively. The high-resolution C1s spectrum of ATP-MPTS-Br was consistent with five different carbon environments owning binding energy at 282.9, 285.0, 286.4, 287.2, and 289.1 ev, which were one by one attributable to the C—Si, C—C/C—H, C—Br, C—O, and C=O. The peak area components were 2425 : 5887 : 1736 : 1813 : 1518, compared with the theoretic ratio (1 : 3 : 1 : 1 : 1), the content of C—Si was much bigger, which was caused by contaminated carbon often appears at lower binding energy, and it was always inevitable [Fig. 2(d) and Table I].

### The characteristic of SI-ATRP of St

The tertiary α-bromoester on the surface of the macroinitiator was known to be an effective initiator for

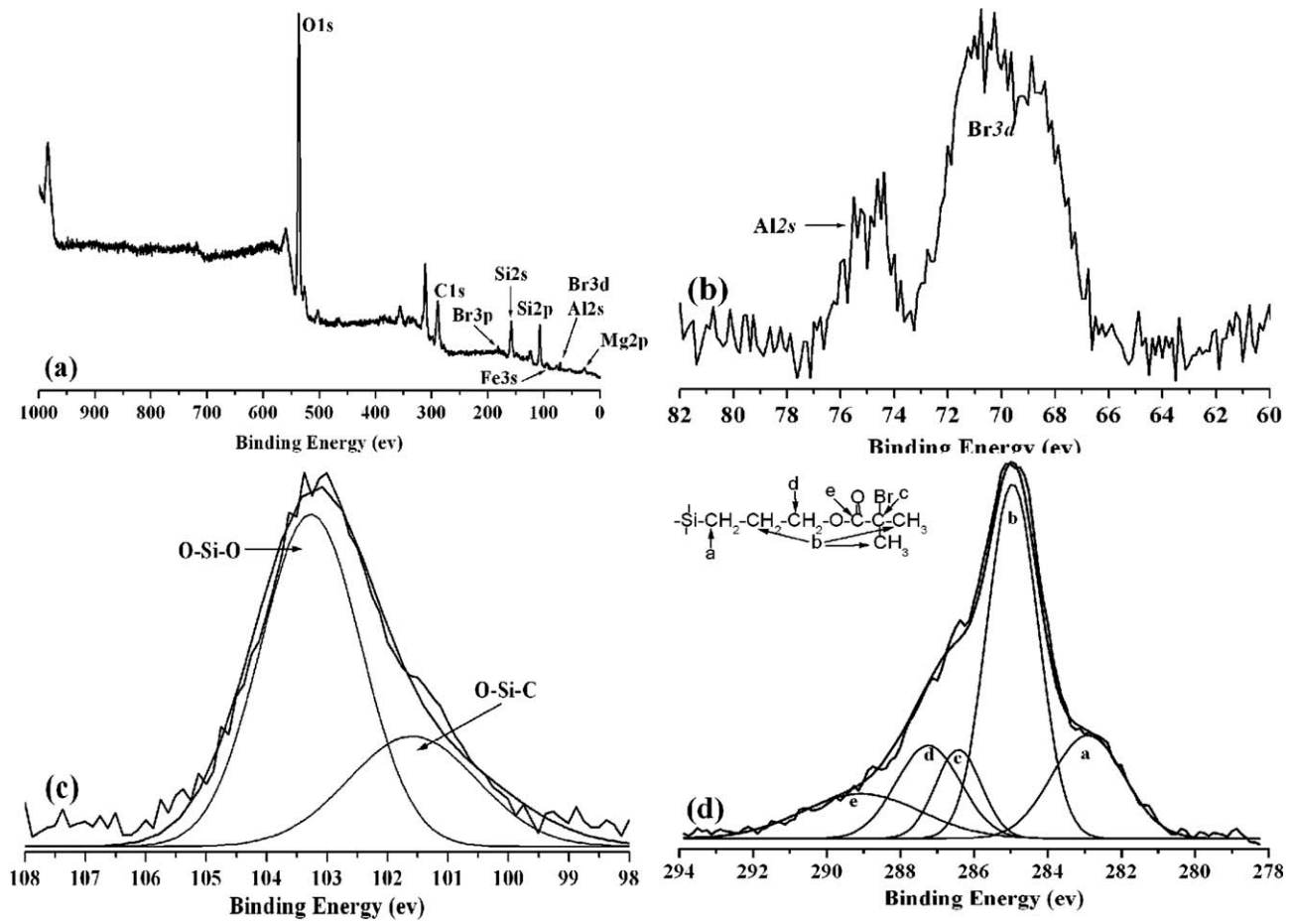


**Figure 2** XPS spectra of the ATP-MPTS-Br: (a) the survey scan spectra, (b) the peak of Br3d, (c) the Si2p core-level spectrum, and (d) the C1s core-level spectrum.

**TABLE I**
**C1s Core-Level Spectrum Parameters for the ATP-MPTS-Br**

| Peaks | Binding energy (ev) | Full-width at half maximum | Peak area |
|---|---|---|---|
| C—Si | 282.9 | 1.96 | 2425 |
| C—C/C—H | 285.0 | 1.38 | 5887 |
| C—Br | 286.4 | 1.24 | 1738 |
| C—O | 287.2 | 1.70 | 1813 |
| O—C=O | 289.1 | 3.20 | 1518 |

ATRP of vinyl monomer.[21] We chose the polymerization time for the early stage and kept the conversion below 40% to study, for the purpose of obtaining the steepest part of the grafting parameter curve and thereby minimizing the effect of the small amount of termination that is unavoidable in controlled/"living" radical polymerization. Because, there was no carbon element in the substrate of ATP particles, it was possible to calculate the conversion of the monomer (C%) and the percentage of the grafting (PG%) from the results of EA. The C% and the PG% were calculated according to the following relationships:

$$\mathrm{C\%} = \frac{\text{PS grafted } (g)}{\text{Monomer used}(g)} \times 100\% \text{ and}$$

$$\mathrm{PG\%} = \frac{\text{PS grafted } (g)}{\text{ATP nanoparticles charged}(g)} \times 100\%$$

As was shown in Figure 3(a), the C% and PG% increased linearly with increasing polymerization time and reached 11.4% and 17.5%, respectively, after a polymerizing time of 12 h. Information about the molecular weight and molecular weight distribution of the grafted polymer were gained by cleaving the ATP cores and subjected to GPC analysis. The plot of number-average molecular weight ($M_n$) and polydispersity (PDI, $M_w/M_n$) against conversion in this polymerization stage were shown in Figure 3(b). A nearly linear increasing in $M_n$ versus monomer conversion was obtained. The PDI values remained low, below 1.25. The Figure 3(a,b) exhibited the characteristics of controlled/"living" polymerization.

### Structure characterization of ATP-*g*-PS

Figure 1(c) showed the FTIR spectra of ATP-*g*-PS. The characteristics bands of PS at 2900–3100 $cm^{-1}$ and the bands of phenyl groups at 700 and 760$cm^{-1}$ were observed, while they were not present in FTIR spectra of the bare ATP and ATP-MPTS-Br [Fig. 1(a,b)]. The presence of the graft PS brush on the surface of ATP nanorods was also verified by XPS analysis. Figure 4 was the C1s core-level spectrum of ATP-*g*-PS, which consisted of a hydrocarbon peak at binding energy of 285.0 ev, an aromatic carbon peak at 284.7 ev and a broad aromatic π-π* shake-up satellites at shift of 6–8 ev from the hydrocarbon peak. Moreover, in this sample, the signals of carboxyl carbon (C=O) peaks are not detected, which are detected in the FTIR analysis of the same sample. It suggested that the carboxyl carbon group exist only inside because the FTIR can analyze more inner chemical structure than the XPS. It is concluded from the result that well-defined polymer chains were grown from the nanoparticle surface to yield an ATP core and a well-defined, densely grafted outer PS layer. The DSC analysis (Fig. 5) was conducted for the ATP-*g*-PS after a polymerizing time of 24 h, and a glass-transition temperature ($T_g$) of PS about 133°C was found. It was higher than the normal one at 102°C [Fig. 6(a) represented the pure PS obtained from the HF extraction of ATP-*g*-PS]. Because the molecular weight of the selected sample

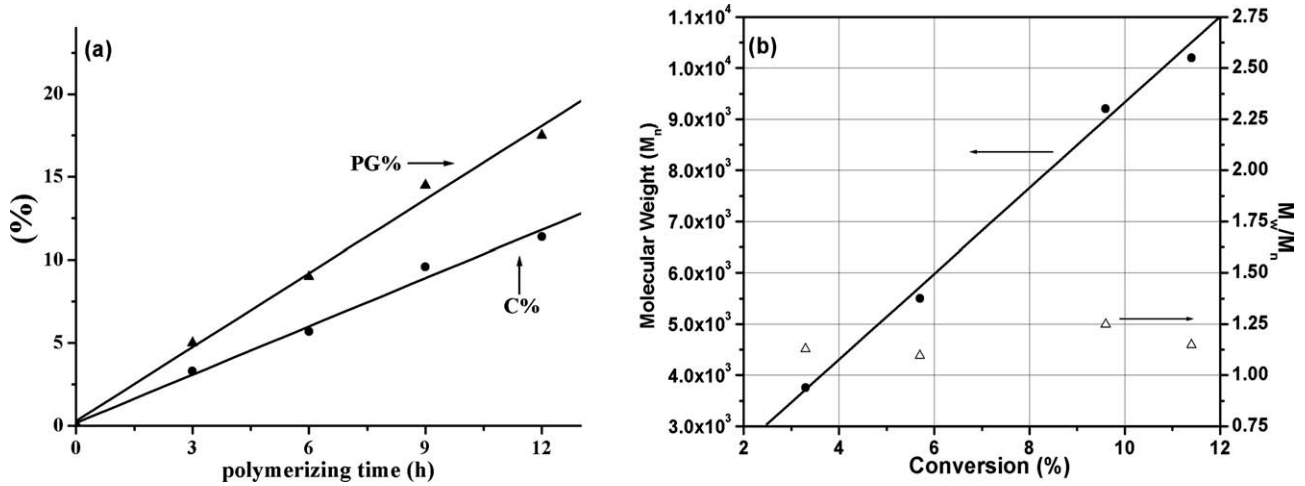


**Figure 3** The characteristic of SI-ATRP of St: (a) the effect of the polymerizing time on the PG% and C% and (b) plots of $M_n$ and $M_w/M_n$ of the cleaved PS versus monomer conversion.

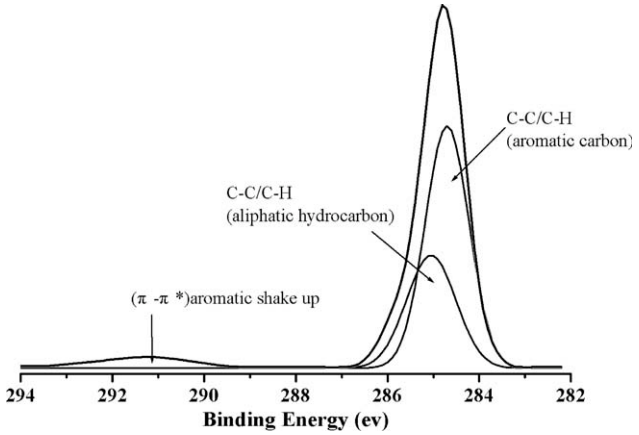


**Figure 4** C1s XPS spectrum of ATP-*g*-PS.

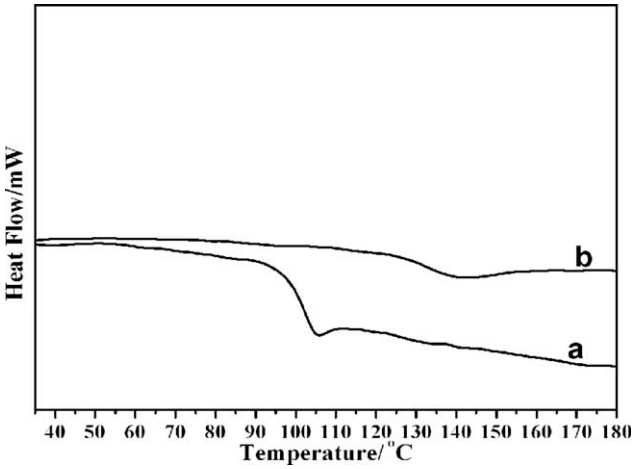


**Figure 5** DSC curve of (a) the PS ($T_g$ = 102°C) and (b) the ATP-*g*-PS ($T_g$ = 133°C).

had no significant difference as judged by GPC studies (usually about 3.2 × $10^4$ g $mol^{-1}$). It was clear that the shift of the $T_g$ only resulted from the nature of the ATP. Because of the extremities of the polymer chain were fixed on the surface of the nanoparticles, the mobility of the PS was hindered, and more energy was needed to pass from a glassy state to a caoutchoutic state thereby increasing the temperature of the glass transition of the PS.[12]

### Morphologies of ATP-*g*-PS particles

Figure 6 showed the TEM micrographs of the nanorods sample cast from dilute toluene solution. In Figure 6(a), it was found that the bare ATP nanorods were serious agglomeration and existing as compact bundles of rod-shaped crystals in the toluene. Figure 6(b) showed the ATP-MPTS-Br, We found that ATP can be separated into dispersed units and had slight soft agglomeration. Because the MPTS-Br was not a good hydrophobic group, it was insufficient to improve and stabilize the dispersion system of ATP-MPTS-Br in toluene. Figure 6(c) represented the ATP-*g*-PS. It could be seen that after surface grafting onto PS, the long and hydrophobic polymer chains could be efficient in preventing ATPs from flocculating, improving its dispersibility in toluene. There was no doubt that our synthetic method for preparing the initiator-coated ATP nanorods was effective to form polymer brush surfaces, which effectively decreased the interfacial tension of the inorganic nanoparticles in organic solvent and thereby thoroughly broke up the soft agglomeration of particles in toluene and promoted their dispersion in organic solvent.

### The characteristics of ATP-*g*-(PS-*b*-PMMA)

To confirm the presence of active chain ends in the PS brushes, we carried out the reinitiation experiment. We used the ATP-*g*-PS as the anchored initiator to SI-ATRP of MMA for building the hybrid nanorods, ATP-*g*-(PS-*b*-PMMA), possessing the block copolymer layer. The cleaved PS-*b*-PMMA from the surface of the ATP particles was measured for GPC analysis. The results were $M_n$ = 13,630 and PDI =

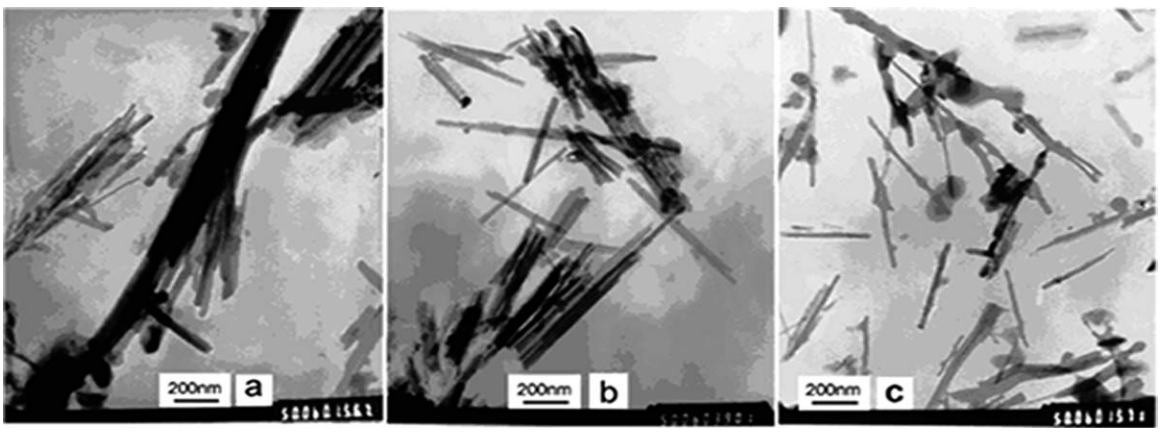


**Figure 6** TEM micrographs of (a) bare ATP, (b) ATP-MPTS-Br, and (c) ATP-*g*-PS.

1.27. The increase of $M_n$ confirmed the presence of living chains ends on the ATP-*g*-PS, and the low PDI proved that the polymerization process had been controlled well. Figure 7 and Table II showed the peak-fitting curve of the C1s peak of block polymer brush on the ATP nanoparticles. Comparing with the C1s spectrum of the ATP-*g*-PS (Fig. 4), we could clearly see that three additional peak at binding energy of 285.8, 287.1, and 289.1 ev, which were attributed to the ester induced β-shifted carbon (C—COO), the methyl side ester (C—O), and the carboxyl carbon (C=O), respectively. Meanwhile, the characteristic peak of PS, the broad aromatic π-π* shake-up satellites, was also observed around 291.5 ev, which indicated the surface of hybrids nanoparticles should contain two kinds of block, PS and PMMA. To analyze quantitatively the surface composition of the brush, the PMMA molar concentration $X$ at the surface was evaluated from the percentage of the carboxyl carbon (C=O) in the C1s envelopes. As in the brush, the relative contribution of PMMA in the C1s intensity was $5X$ (five carbon atom per PMMA repeat unite) and that of PS was $8(1 - X)$ (eight carbon atom per PS repeat unite), we had

$$\frac{A_{C=O}}{A_C} = \frac{X}{5X + 8(1 - X)} \text{ rearranging, gives :}$$

$$X = \frac{8A_{C=O}/A_C}{1 + 3A_{C=O}/A_C} \times 100\%$$

where $X$ was the molar PMMA surface concentration in the brush, and $A_C$ and $A_{C=O}$ were the areas of the C1s envelopes and ester peak, respectively. The ester peak at 289.1 ev was specifically chosen, because it did not significantly overlap any other peak and contained contribution solely from PMMA. According to the data of Table II, in the case of our experiment, the area ratio of the ester peak carbonyl to the C1s envelopes was found 6.4% in the ATP-*g*-(PS-*b*-PMMA) brush. Therefore, the PMMA molar concentration at the surface brush was 43%. In other words, although there was long polymerization time for the second block (24 h), the surface was not completely covered with the second layer of polymer.

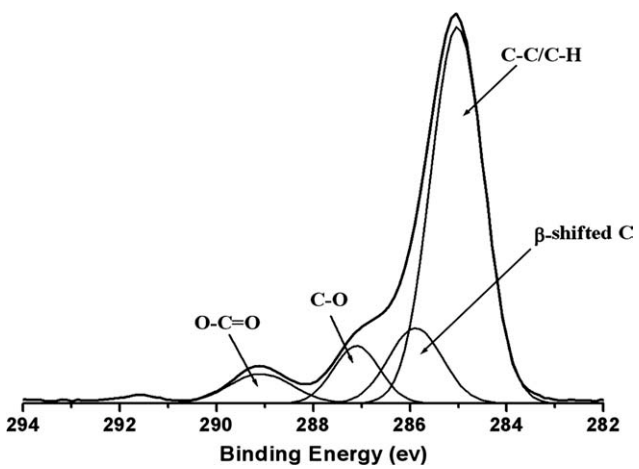


**Figure 7** C1s XPS spectrum of ATP-*g*-(PS-*b*-PMMA).

**TABLE II**
**C1s Core-Level Spectrum Parameters for the ATP-g-(-PS-b-PMMA)**

| Peaks | Binding energy (ev) | Full-width at half maximum | Atomic % (peak area) |
|---|---|---|---|
| C—C/C—H | 285.0 | 1.10 | 70.7 (21690.3) |
| β-shifted C | 285.8 | 1.11 | 13.8 (4240.5) |
| C—O | 287.1 | 1.05 | 9.0 (2766.7) |
| O—C=O | 289.1 | 1.31 | 6.4 (1962.4) |

## CONCLUSIONS

In summary, we have demonstrated a practical method to the facial synthesis of thick-coated polymer-nanoparticles. The macroinitiator for ATRP was obtained via simply modified ATP nanorods and immobilized tertiary α-bromoester on its surface. Polymerization of St using ATP nanorod initiators displayed the diagnostic criteria for a controlled/"living" radical polymerization, and the ATP-*g*-PS might be used as a macroinitiator to build block copolymer. Well-defined polymer chains were grown from the nanoparticle surface to yield individual nanorods composed of an ATP core and a well-defined, densely grafted outer PS or PS-*b*-PMMA layer. Different from the spherical or quasi-spherical cores reported, the needle-shaped particle has larger specific surface area so that it is very difficult to be stabilized in the organic solvent, the system is more fragile, and the needles are easy to fall out. Here, structurally well-defined, densely grafted, and hydrophobic polymer core@shell structurer by SI-ATRP could be obtained.

## References

1. Gachkovskii, V. F. Adv Mol Relax Proc 1973, 5, 245.
2. Gachkovskii, V. F.VySokomol Soed 1965, A7, 2009.
3. Ma, J.;Ramelow, U. S.;Tauber, J. D. Tr J Chem 1997, 21, 313.
4. Diaz, A. F.;Castillo, J. I.;Logan, T. A.;Lee, W. J. J Electroanal Chem 1981, 129, 115.
5. Pellagrino, J.;Radebaugh, R.;Mattes, B. R. Macromolecules 1996, 29, 4985.
6. Peres, R. C. O.;De Paoli, M. A. J Power Sources 1992, 40, 299.
7. Selampinar, F.;Akbulut, U.;Orden, M. Y.;Toppare, L. Biomaterials 1997, 92, 1163.
8. Kizilyar, N.;Orden, N, Y.;Toppare, L.;Yager, Y. Synth Mat 1999, 104, 45.
9. Ramelow, U. S.;Ma, J.;Darbeau, R. Mat Res Innovat 2001, 5, 40.
10. Ramelow, U. S.;Braganza, S. N.;Ramelow, G. J Appl Polym Sci 2009, 112, 1916.

11. Wang, H. L.;Toppare, L.;Ferondes, J. E. Macromolecules 1990, 23, 1053.
12. Yurtsever, M.;Toppare, L. Polymer 1990, 40, 5459.
13. McKellar, J. F.; Allen, N. S. Photochemistry of Man-Made Polymers; Applied Science Publishers LTD: London, 1979, p 276.
14. Anderson, B. C.; Lipsomb, R. D. Macromolecules 1984, 17, 1641.
15. Ogawa, T.; Cedeno, R.; Herrera, E. T. Macromol Chem 1979, 180, 185.
16. Ogawa, T.; Cedeno, R.; Inoue, M. Polym Bull 1980, 2, 275.
17. Ogawa, T.; Cedeno, R.; Herrera, T. E. Amanoz, B.; Inoue, M. In Conductive Polymers; Seymour, R.B, Ed.; Plenum Press: New York and London, 1981; Vol.15, p 85.
18. Chem 451 Final Report, Fall 2009, McNeese State University, Department of Chemistry, Lake Charles, LA 70609.
19. Ramelow, S. U.; Wagle, R. J Appl Polym Sci 2011, 119, 1469.
20. Brandrup, J.; Immergut, E. H. The Polymer Handbook; Wiley Interscience: New York, NY, 1966.
21. Rodney, J. Sime. Physical Chemistry: Methods, Techniques and Experiments; (Saunders golden Sunburst series) Harcourt Brace College Publishers, New York, 1990, 687.
22. Herzfeld, K. F.; Sklar, A. L. Rev Mod Phys 1942, 14, 294.
23. Shoemaker, D. P.; Garland, C. W.; Nibler, J. W. Experiments in Physical Chemistry, 7th ed.; McGraw Hill, New York, 2003, 380.
24. Kuhn, H.; J Chem Phys 1949, 17, 1198;Kuhn, H.; Fortch Chem Organ Naturstoffe 1959, 17, 404.
25. Chang, R. Basic Principles of Spectroscopy; McGraw Hill: New York, 1971.